



Electrochemical deposition and characterization of Ni-Mo alloy powders

M.G. Pavlović¹, B.M. Jović², V.D. Jović², U. Lačnjevac^{2*}, V.M. Maksimović³

¹*Institute of Electrochemistry ICTM, 11000 Belgrade, Njegoševa 12, Serbia,*

²*Center for Multidisciplinary Studies University of Belgrade, 11030 Belgrade, P.O.Box 33, Serbia,*

³*Institute of Nuclear Sciences Vinča, 11001 Belgrade, P.O.Box 522, Serbia*

Received 4 September 2007; received in revised form 23 October 2007; accepted 7 November 2007

Abstract

Electrodeposition of Ni-Mo alloy powders from ammonium sulfate and ammonium chloride containing electrolytes of different Ni/Mo ions concentration ratios was investigated by polarization measurements. The morphology, chemical composition and phase composition of electrodeposited Ni-Mo alloy powders were investigated using DSC, TGA, SEM, EDS and XRD analysis. EDS results showed that powder composition depends on Ni/Mo ions concentration ratio, as well as on the position where the EDS analysis was performed. As-deposited alloy powders were nanocrystalline showing no XRD peaks with undefined morphology (SEM). After recrystallization for 2 h in N₂ atmosphere at 600°C the presence of NiMoO₄ phase was identified in the powder electrodeposited from chloride electrolyte at the Ni/Mo ions concentration ratio 1/3, with well defined crystalline powder particles.

Keywords: electrodeposition, Ni-Mo alloy powder, morphology, phase composition

1. Introduction

Nickel-molybdenum alloys possess several useful properties, while their catalytic activity for hydrogen evolution was one of the most investigated property in the literature [1–8].

Ni-Mo alloys can be produced by several methods, from which metallurgical ones are not convenient because of easy oxidation and high melting temperature of molybdenum. Powder metallurgy and mechanical alloying [9,10], spark plasma sintering [11] and laser cladding [12] are mostly used for Ni-Mo alloy preparation. All above mentioned methods are expensive in comparison with the electrodeposition of Ni-Mo alloy coatings. Although molybdenum cannot be separately deposited from aqueous solutions, it can be co-deposited with the iron-group metals (Fe, Ni, Co) in the presence of appropriate complexing agents, by the type of alloy deposition defined by Brenner [13] as induced co-deposition.

Most of the papers concerning electrodeposition of compact Ni-Mo alloy coatings are dealing with the mechanism of their deposition (mechanism of induced co-deposition) [14–17].

Only a few papers are devoted to morphological and phase composition characterization of these alloys [18–21]. It was found by XRD analysis that Ni-Mo alloys electrodeposited from citrate bath (pH 8.5–9.5) contain NiMo solid solution, with diffraction peaks being sharp at lower content of Mo (up to 12 wt%) and wide at high content of Mo (30 wt%) [20]. In the same paper TEM revealed the same solid solution with the grain size ranging between 4 nm and 17 nm (average 5 nm). Similar conclusion was made by the XRD analysis of Ni-Mo alloys electrodeposited from pyrophosphate-ammonium chloride bath (pH 8.5) [21]. It was also demonstrated by EDS analysis [18,19] that electrodeposited Ni-Mo alloys with higher amount of Mo contain up to about 50 at% of oxygen. XRD showed sharp diffraction peaks corresponding to Ni-Mo solid solution and Ni₄Mo intermetallic compound [19], while XPS analysis revealed that in the alloy with higher amount of Mo, among metallic Mo, a mixture of polyvalent molybdenum oxides or hydroxides, mainly in the form of Mo (V) and Mo (IV) is present in the deposit.

* Corresponding author: tel. +381 11 208 5039; fax. +381 11 305 5289, E-mail: uroslacnjevac@yahoo.com

It should be emphasized here that there are no papers in the literature concerning electrodeposition of Ni-Mo alloy powders and their characterization.

In this paper an attempt was made to investigate the process of Ni-Mo alloy powders electrodeposition from ammonium sulfate and ammonium chloride containing electrolytes, as well as their morphology, chemical composition and phase composition.

II. Experimental Procedure

Polarization diagrams were recorded in a three-compartment standard electrochemical cell at the temperature of $25 \pm 1^\circ\text{C}$. The platinum foil counter electrode and the reference– saturated silver/silver chloride, Ag|AgCl – electrode ($E_{\text{ref}} = 0.20\text{ V vs. NHE}$) were placed in separate compartments. The latter was connected to the working electrode by a Luggin capillary positioned at the distance of 0.2 cm from the working electrode surface. The working electrodes were either glassy carbon or Ni rod ($d = 0.3\text{ cm}$) sealed in epoxy so that only the surface area of the disc of 0.071 cm^2 was exposed to the solution and was placed parallel to the counter electrode in a vertical position. Before each experiment working electrode surface was polished down to $0.05\ \mu\text{m}$ alumina impregnated polishing cloths, cleaned in an ultrasonic bath for 10 min., thoroughly washed with distilled water and transferred to the electrochemical cell.

Polarization measurements were performed by a computer-controlled potentiostat (PAR M273A) using

the corrosion software (PAR M352/252, version 2.01) with the sweep rate of 1 mV s^{-1} . For obtaining polarization curves corrected for IR drop, current interrupt technique was used with time of current interruption being 0.5 s.

All powders were electrodeposited at the room temperature in the cylindrical glass cell of the total volume of 1 dm^3 with cone shaped bottom of the cell in order to collect powder particles. Ni-Mo alloys were deposited under galvanostatic conditions on Ni or glassy carbon cylinder ($d = 0.5\text{ cm}$, $h = 3\text{ cm}$) at appropriate limiting current density. All solutions were made from analytical grade purity chemicals and distilled water. Details of the conditions for powders electrodeposition are given in Table 1.

The morphology of the electrodeposited powders was examined using scanning electron microscopes (SEM), JEOL JSM–6460LV equipped with an energy-dispersive X-ray spectroscopy (EDS), Oxford Instruments INCA X-sight system and Tescan VEGA TS 5130MM.

The thermal behavior of powders was investigated from room temperature to 900°C using an SDT Q600 simultaneous DSC-TGA analyzer (TA Instruments) and alumina crucibles with a heating rate of $20^\circ\text{C min}^{-1}$ under a dynamic N_2 atmosphere.

The phase composition of the powders was investigated using a PHILIPS PW 1050 X-ray powder diffractometer.

Table 1. Main characteristics of the electrolytes and conditions of powders electrodeposition

Sample No.	Working electrode	Ni/Mo	Ni^{2+} [M]	Bath composition (Bath No.)	pH	J_{dep} [A cm^{-2}]
1	Ni	1/2	0.02	0.02M NiSO_4 ; 0.04M Na_2MoO_4 1M $(\text{NH}_4)_2\text{SO}_4$; 0.7M NH_4OH (B1)	9.4	1.1 ^a
2	Ni	1/6	0.02	0.02M NiSO_4 ; 0.12M Na_2MoO_4 1M $(\text{NH}_4)_2\text{SO}_4$; 0.7M NH_4O (B2)	9.4	1.1 ^a
3	Ni	1/1	0.1	0.1M NiCl_2 ; 0.1M Na_2MoO_4 1M NH_4Cl ; 0.7M NH_4OH (B3)	9	0.5 1.1 ^a
4	Glassy Carbon	1/0.5	0.1	0.1M NiCl_2 ; 0.05M Na_2MoO_4 1M NH_4Cl ; 0.7M NH_4OH (B4)	9	1.3 ^a
5	Glassy Carbon	1/1	0.1	0.1M NiCl_2 ; 0.1M Na_2MoO_4 1M NH_4Cl ; 0.7M NH_4OH (B4)	9	2.3 1.2 ^a
6	Glassy Carbon	1/3	0.1	0.1M NiCl_2 ; 0.3M Na_2MoO_4 1M NH_4Cl ; 0.7M NH_4OH (B5)	9	1.2 ^a
7	Glassy Carbon	2/1	0.2	0.2M NiCl_2 ; 0.1M Na_2MoO_4 1M NH_4Cl ; 0.7M NH_4OH (B7)	9	1.6 ^a

^aThe current density corresponding to point B on Fig. 1.

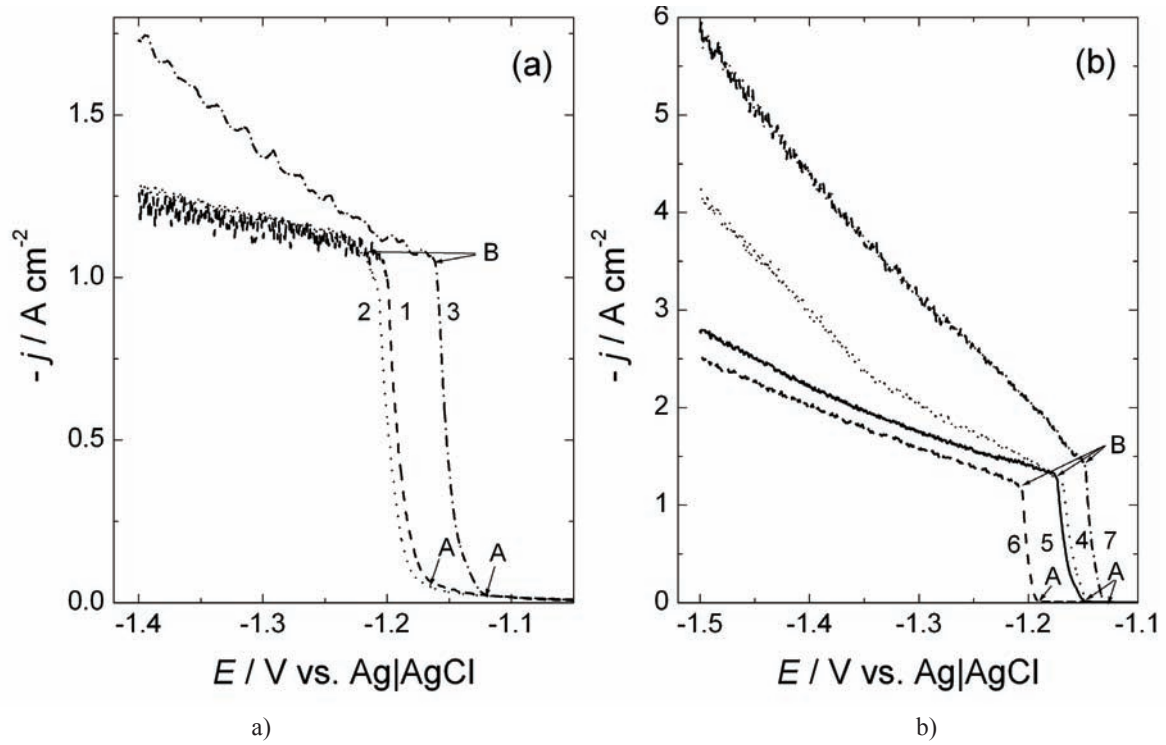


Figure 1. Polarization diagrams for Ni-Mo powders electrodeposition onto Ni electrode (a) and onto glassy carbon electrode (b) Numbers of powder samples are marked in the figure (see Table 1).

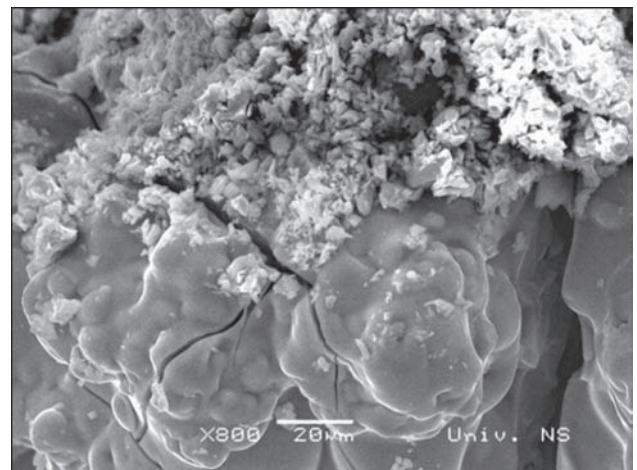
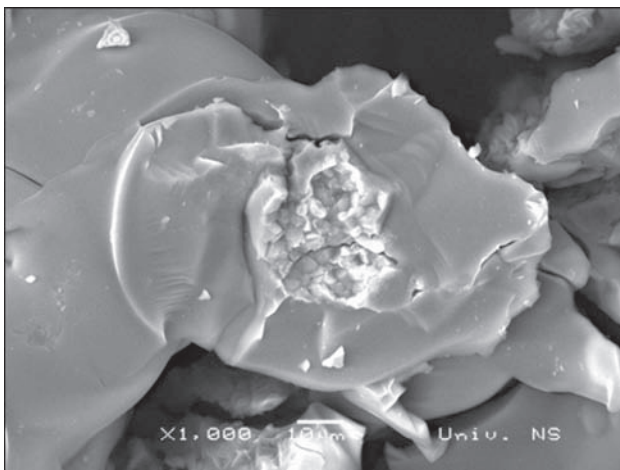
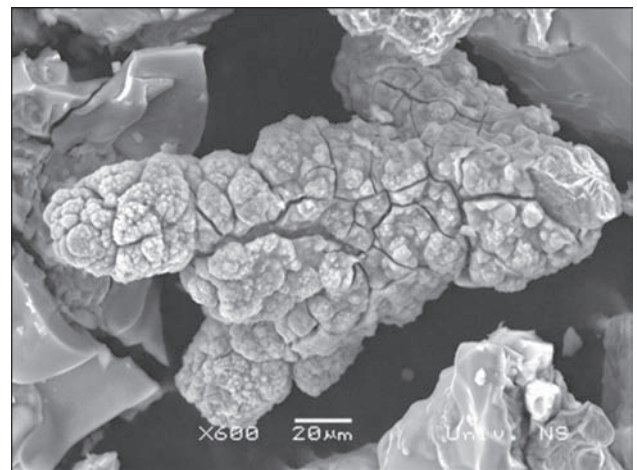
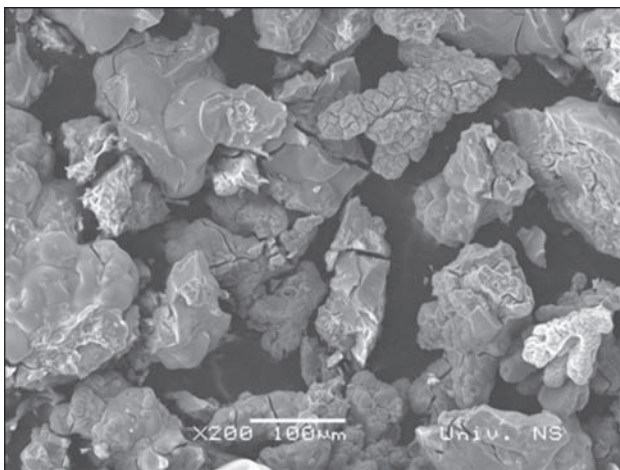


Figure 2. Morphology of as-deposited powders obtained from sulfate electrolytes onto Ni electrode (samples 1 and 2)

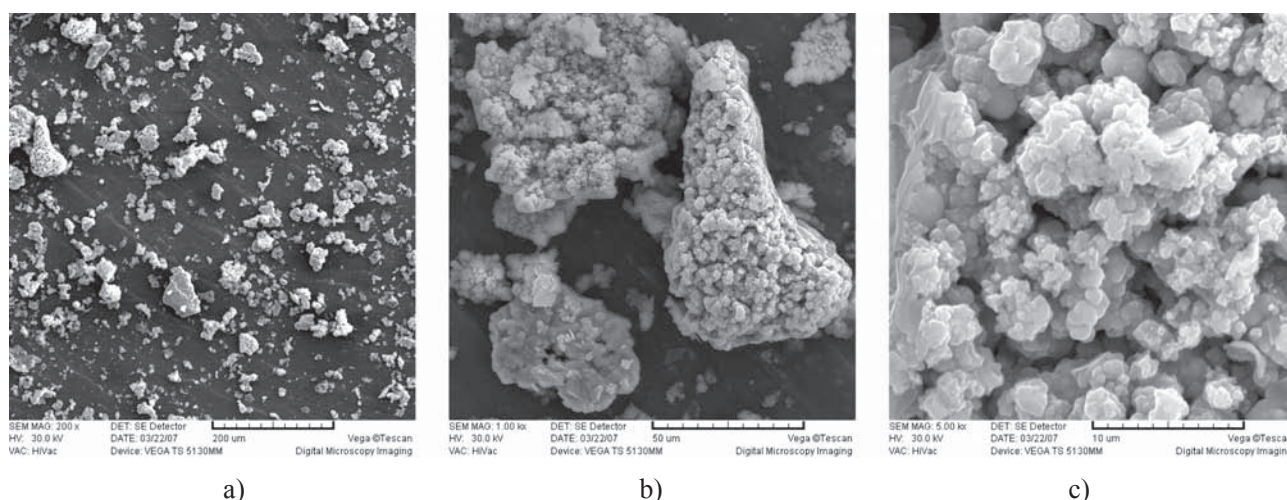


Figure 3. Morphology of as-deposited powders obtained from chloride electrolytes onto glassy carbon electrode (sample 4)

III. Results and Discussion

Polarization measurements

Polarization curves recorded in different baths (see Table 1) are shown in Fig. 1. As can be seen similar shapes of polarization curves recorded onto Ni (a) and glassy carbon (b) electrodes are obtained, characterized by two inflection points. The first inflection point (A) reflects the beginning of alloy deposition, while the second one (B) corresponds to the moment when the deposition process is controlled by the rate of hydrogen bubble formation (explained in our previous papers [22,23]). It is important to note that the potential of the beginning of alloy deposition (A) becomes more negative with the increase of molybdenum ions concentration (with the decrease of Ni/Mo ratio) in both solutions, which is in accordance with the theory of induced co-deposition [13]. At the same time much higher current densities are recorded for electrodeposition of Ni-Mo alloys from chloride containing electrolytes on glassy carbon electrode (Fig. 1b). Such a behavior is most likely due to more pronounced nucleation on foreign substrate (glassy carbon) in comparison with the Ni electrode (where usually epitaxial growth occurs). Growth of separate nuclei, followed by their transformation into dendrites, causes formation of rougher surface and accordingly higher current density of alloy electrodeposition. At the same time the presence of different anions, having different dimensions and adsorption properties, could also influence the process of Ni-Mo alloy electrodeposition, causing different values of current density.

It should also be mentioned that the current efficiency for alloy deposition in all cases is very low, up to 5%.

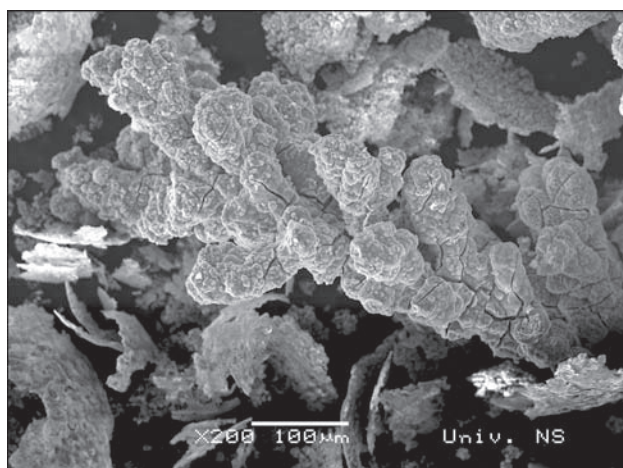
Morphology of as-deposited powders

All powders for morphological, compositional and phase composition analysis were deposited at the val-

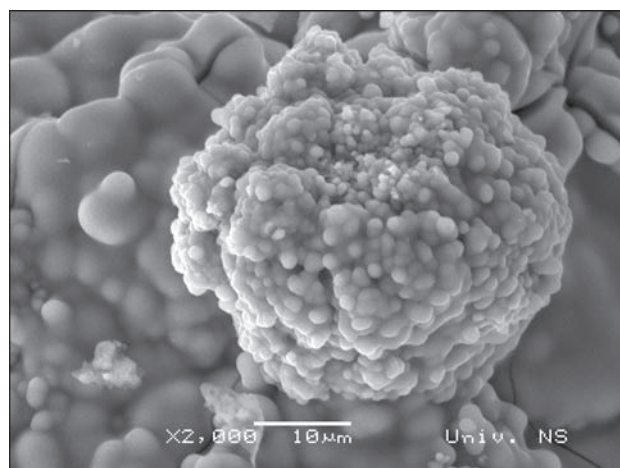
ue of the current density corresponding to the inflection point B (see Table 1), except powder samples 3 and 5 which were deposited at two values of the current density. In the case of powder sample 3 the deposition current density was set at a half of the one corresponding to point B, while in the case of the sample 5 the deposition current density was set at a higher value than that of point B, in order to determine the influence of the current density on the morphology. No influence of the current density on the morphology of sample 5, deposited either at the current density of point B or at higher current density (Table 1), was detected. In the case of the sample 3, more pronounced presence of a compact deposit was detected for current density of 0.5 A cm^{-2} than for that corresponding to the point B (1.1 A cm^{-2}). The morphology of as-deposited powders depends on the material of working electrode, the presence of anions, as well as on the Ni/Mo concentration ratio.

Powder particles electrodeposited onto Ni from sulfate electrolyte are shown in Fig. 2. As can be seen (Fig. 2a) size of the particles vary in the range 20–200 μm and all of them are characterized by the presence of cracks (Fig. 2b-d). Two types of particles are detected: cauliflower type particles (Fig. 2a,b) and particles characterized with flat and rounded edges (Fig. 2c,d).

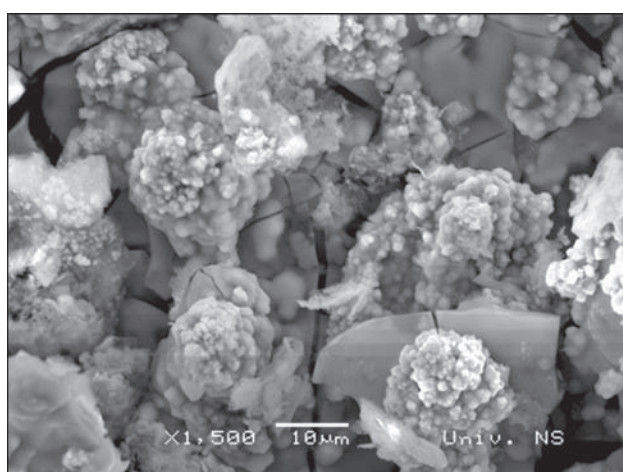
Powder particles electrodeposited onto glassy carbon from chloride electrolyte are shown in Figs. 3 and 4. As can be seen (Fig. 3a,b) size of the particles is smaller in comparison with those electrodeposited from sulfate electrolyte, varying in the range 5–50 μm . Their morphology is found to depend on the Ni/Mo concentration ratio. At the highest Ni/Mo ratio of 1/0.5 (Fig. 4b,c) cracks are not present on the particles and crystalline structure could be detected on the top surface of the particles. With the decrease of the Ni/Mo ratio (1/1) cauliflower type particles (Fig. 4a) with rounded edges (Fig. 4b) are obtained characterized with the presence



a)



b)



c)

Figure 4. Morphology of as-deposited powders obtained from chloride electrolytes onto glassy carbon electrode: (a, b – sample 5; c – sample 6)

of cracks. In the case of Ni/Mo ratio of 1/3 (Fig. 4c) flat and thin parts of the particles are covered with rounded agglomerates and cracks are more pronounced. The appearance of large number of cracks is the results of high tensile stresses present in the powder and the hydrogen evolution [20].

Approximate composition of as-deposited powders

The approximate compositions of all alloy powders, evaluated by EDS microanalysis, are given in Table 2. It was found that the composition not only depends on Ni/Mo concentration ratio, but also on the position of the powder particle at which the EDS analysis was performed. These results indicate the presence of significant amount of oxygen in the powders, as well as the non-homogeneous composition of as-deposited powders.

XRD analysis of as deposited and recrystallized powder

Phase composition analysis of the powders was performed using XRD. The results show that no peaks are detected on as-deposited powders (except one halo observed near $2\theta = 44^\circ$ (see Fig. 5 – amorphous), since the crystallites were extremely small, i.e. of the order of nanometer. It was obvious that Ni-Mo alloy powders should be previously recrystallized in order to determine their phase composition. Before recrystallization sample 6 was analyzed by DSC and TGA in order to determine recrystallization temperature. As can be seen in Fig. 6 sharp peak on the DSC curve at 543°C indicates that recrystallization should be performed at

Table 2. Approximate composition of Ni-Mo alloy powders as a function of Ni/Mo ions ratio, type of the bath and the position of EDS electron beam at the powder particle

Bath No.	Ni/Mo	at % O ₂	at % Ni	at % Mo
B1	1/2	69	5	26
		79	1	20
B2	1/6	86	1	13
		67	4	29
B3	1/1*	81	3	15
B3	1/1	60	18	22
		51	16	33
B6	1/3	66	16	18

* Working electrode: Ni

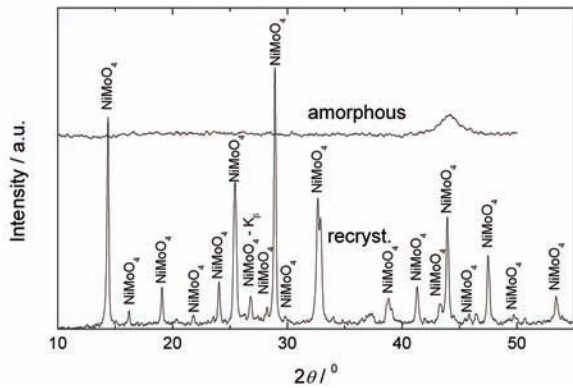


Figure 5. XRD of powder sample 6 before (amorphous) after recrystallization (recryst.)

this or higher temperature. Recrystallization was performed in N_2 atmosphere at $600^\circ C$ for 2 h. XRD analysis revealed structural transformation and formation of $NiMoO_4$ phase in the powder, as can be seen in Fig. 5 (recryst.). With the exception of a few small peaks, all other peaks correspond to the $NiMoO_4$.

The example of the recrystallized powder (sample 6) particles is shown in Fig 7. The regular crystals are obtained with smooth surfaces (Fig. 7b) and well defined crystal planes. The size of particles is seen to be much smaller ($< 5 \mu m$, Fig. 7a) than the size of as deposited particles, indicating that during the process of recrystallization agglomerates formed during electrodeposition separate into much smaller crystals. Such a change is most likely the consequence of a possible chemical reaction occurring during the process of recrystalliza-

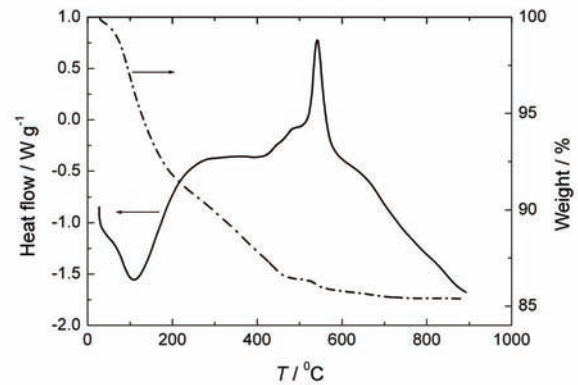


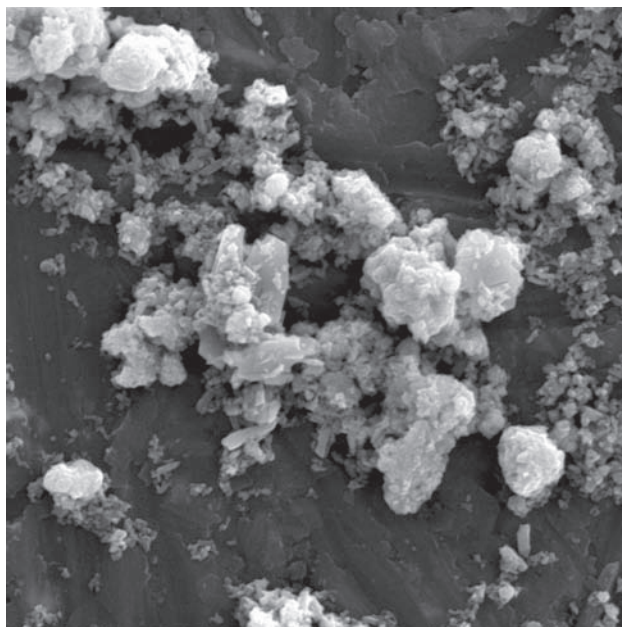
Figure 6. DSC and TGA of powder sample 6 phase, indicating that it is possible to obtain single phase Ni-Mo powder by electrochemical deposition

tion (annealing), indicated by a small peak positioned at about $490^\circ C$ on the DSC curve (Fig. 6).

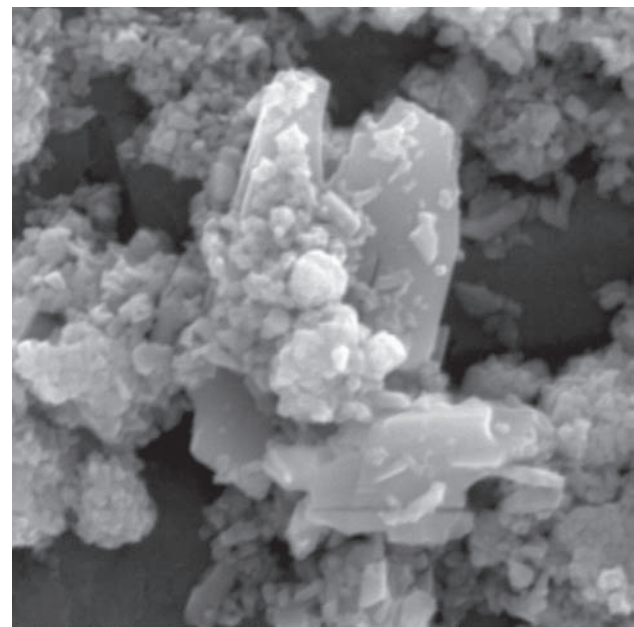
IV. Conclusions

The morphology and composition of obtained powders depend on the anion present in the solution, material of the working electrode, as well as on the Ni/Mo ions concentration ratio. However, according to EDS results the chemical composition of powder is not homogeneous. XRD analysis reveals that the alloy powder has crystalline structure after recrystallization with the presence of single $NiMoO_4$ phase in the powder electrodeposited at Ni/Mo ratio 1/3 from chloride electrolyte onto glassy carbon electrode.

Acknowledgements: This work was financially supported by Ministry of Science and Environmen-



a)



b)

Figure 7. Morphology of recrystallized powder of sample 6

tal Protection of the Republic of Serbia through Project no.142032G/2006. The authors are indebted to Prof. D. Poleti from the Faculty of Technology and Metallurgy University of Belgrade for useful discussions and DSC–TGA analysis.

References

1. B.E. Conway, L. Bai, D.F. Tessier, “Data collection and processing of open-circuit potential-decay measurements using a digital oscilloscope: Derivation of the H-capacitance behaviour of H₂-evolving, Ni-based cathodes”, *J. Electroanal. Chem.*, **161** (1984) 39–49.
2. B.E. Conway, L. Bai, M.A. Sattar, “Role of the transfer coefficient in electrocatalysis: Applications to the H₂ and O₂ evolution reactions and the characterization of participating adsorbed intermediates”, *Int. J. Hydrogen Energy*, **12** (1987) 607–621.
3. I.A. Raj, K.I. Vasu, “Transition metal-based cathodes for hydrogen evolution in alkaline solution: Electrocatalysis on nickel-based ternary electrolytic codeposits”, *J. Appl. Electrochem.*, **22** (1992) 471–477.
4. C. Fan, D.L. Piron, P. Paridis, “Hydrogen evolution on electrodeposited nickel-cobalt-molybdenum in alkaline water electrolysis”, *Electrochim. Acta*, **39** (1994) 2715–2722.
5. M.R. Gennero de Chialvo, A.C. Chialvo, “Hydrogen evolution reaction on smooth Ni (1-x) + Mo (x) alloys (0 ≤ x ≤ 0.25)”, *J. Electroanal. Chem.*, **448** (1998) 123–141.
6. J. Divisek, H. Schmotz, J. Balej, “Ni and Mo coatings as hydrogen cathodes”, *J. Appl. Electrochem.*, **19** (1989) 519–530.
7. A. Lasia, A. Rami, “Kinetics of hydrogen evolution on nickel electrodes”, *J. Electroanal. Chem.*, **294** (1990) 123–141.
8. J.M. Jakšić, M.V. Vojnović, N.V. Krstajić, “Kinetic analysis of hydrogen evolution at Ni–Mo alloy electrodes”, *Electrochim. Acta*, **45** (2000) 4151–4158.
9. P. Kedzierzawski, D. Oleszak, M. Janik-Czachor, “Hydrogen evolution on hot and cold consolidated Ni–Mo alloys produced by mechanical alloying”, *Mater. Sci. Eng.*, **A300** [1–2] (2001) 105–112.
10. D. Oleszak, V.K. Portnoy, H. Matyja, “Structure of mechanically alloyed Ni–Mo powders”, *Mater. Sci. Forum*, **312** (1999) 345–350.
11. S.D. De la Torre, D. Oleszak, A. Kakitsuji, K. Miyamoto, H. Miyamoto, S.R. Martinez, C.F. Almeraya, V.A. Martinez, J.D. Rois, “Nickel-molybdenum catalysts fabricated by mechanical alloying and spark plasma sintering”, *Mater. Sci. Eng.*, **A276** [1–2] (2000) 226–235.
12. G.L. Goswami, S. Kumar, R. Galun, B.L. Mordike, “Laser cladding of Ni–Mo alloys for hardfacing applications”, *Lasers Eng.*, **13** [1] (2003) 1–6.
13. A. Brenner, *Electrodeposition of Alloys*, Vol. II. Academic Press Inc. New York, 1963.
14. E.J. Podlaha, D. Landolt, “Induced codeposition. I. An experimental investigation of Ni–Mo alloys”, *J. Electrochem. Soc.*, **143** (1996) 885–892.
15. E.J. Podlaha, D. Landolt, “Induced codeposition. II. Mathematical model describing the electrodeposition of Ni–Mo alloys”, *J. Electrochem. Soc.*, **143** (1996) 893–899.
16. E.J. Podlaha, D. Landolt, “Induced codeposition. III. Molybdenum alloys with nickel, cobalt, and iron”, *J. Electrochem. Soc.*, **144** (1997) 1672–1680.
17. A. Marlot, P. Kern, D. Landolt, “Pulse plating of Ni–Mo alloys from Ni-rich electrolytes”, *Electrochim. Acta*, **48** (2002) 29–36.
18. L.S. Sanches, S.H. Domingues, A. Carubelli, L.H. Mascaro, “Electrodeposition of Ni–Mo and Fe–Mo alloys from sulfate-citrate acid solutions”, *J. Braz. Chem. Soc.*, **14** (2003) 556–563.
19. L.S. Sanches, S.H. Domingues, C.E.B. Marino, L. H. Mascaro, “Characterization of electrochemically deposited Ni–Mo alloy coatings”, *Electrochem. Comm.*, **6** (2004) 543–548.
20. E. Chassaing, N. Portail, A.F. Levy, G. Wang, “Characterization of electrodeposited nanocrystalline Ni–Mo alloys”, *J. Appl. Electrochem.*, **34** (2004) 1085–1091.
21. M. Donten, H. Cesiulis, Z. Stojek, “Electrodeposition of amorphous/nanocrystalline and polycrystalline Ni–Mo alloys from pyrophosphate baths”, *Electrochim. Acta*, **50** (2005) 1405–1412.
22. V.D. Jović, B.M. Jović, M.G. Pavlović, “Electrodeposition of Ni, Co and Ni–Co alloy powders”, *Electrochim. Acta*, **51** (2006) 5468–5477.
23. V.D. Jović, B.M. Jović, V. Maksimović, M.G. Pavlović, “Electrodeposition and morphology of Ni, Co and Ni–Co alloy powders. Part II: Ammonium chloride supporting electrolyte”, *Electrochim. Acta*, **52** (2007) 4254–4263.